

# Multi-View Projection for Unsupervised Domain Adaptation in 3D Semantic Segmentation

Andrew Caunes<sup>1,2</sup>, Thierry Chateau<sup>1</sup>, and Vincent Frémont<sup>2</sup>

<sup>1</sup> Logiroad, Nantes, France

<sup>2</sup> LS2N - Ecole Centrale de Nantes, France

**Abstract.** 3D semantic segmentation plays a pivotal role in autonomous driving and road infrastructure analysis, yet state-of-the-art 3D models are prone to severe domain shift when deployed across different datasets. In this paper, we propose an Unsupervised Domain Adaptation approach where a 3D segmentation model is trained on the target dataset using pseudo-labels generated by a novel multi-view projection framework. Our approach first aligns Lidar scans into coherent 3D scenes and renders them from multiple virtual camera poses to create large-scale synthetic 2D semantic segmentation datasets in various modalities. The generated datasets are used to train an ensemble of 2D segmentation models in point cloud view domain on each modality. During inference, the models process a large amount of views per scene; the resulting logits are back-projected to 3D with a depth-aware voting scheme to generate final point-wise labels. These labels are then used to fine-tune a 3D segmentation model in the target domain. We evaluate our approach Real-to-Real on the nuScenes and SemanticKITTI datasets. We also evaluate it Simulation-to-Real with the SynLidar dataset. Our contributions are a novel method that achieves state-of-the-art results in Real-to-Real Unsupervised Domain Adaptation, and we also demonstrate an application of our method to segment ‘rare classes’, for which target 3D annotations are not available, by only using 2D annotations for those classes and leveraging 3D annotations for other classes in a source domain.

**Keywords:** 3D Semantic Segmentation · Unsupervised Domain Adaptation · Autonomous Driving · Lidar · Multi-view Projection

## 1 Introduction

3D semantic segmentation of Lidar scenes is crucial for applications such as autonomous driving (AD) and road infrastructure analysis. In particular, many applications require models to be able to generalize to unseen data, which may not be from the same domain as the training data, e.g. if the data was acquired in a different location or with a different sensor. The main approach to mitigate this problem is Unsupervised Domain Adaptation (UDA).

Most existing methods are tailored for AD, thus making concessions on accuracy to guarantee real-time performance on single or few Lidar scans [24,23,18,30].

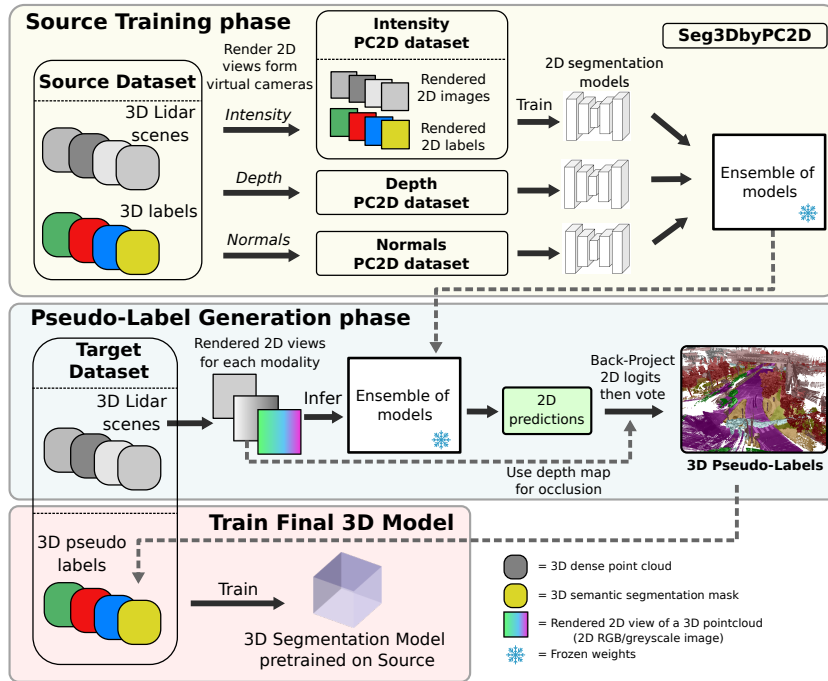


**Fig. 1. Overview of Seg3DbyPC2D .** Unsupervised Domain Adaptation for 3D semantic segmentation is achieved by fine-tuning a 3D model pretrained on the source dataset on pseudo-labels generated for the target domain. To generate these pseudo-labels, a multi-view projection method is used. *Source Training Phase (yellow)*. First, starting from 3D scenes (LiDAR scans accumulated in a common frame) and 3D segmentation masks, virtual camera poses are sampled around each scene. 2D images along with 2D segmentation masks are then rendered from the poses in a chosen modality (e.g. Lidar intensity colors). See Fig. 2 for details on this dataset generation step. Each generated dataset is then used to train an individual 2D semantic segmentation model, which together form an ensemble. *Pseudo-label generation phase (blue)*. For each target 3D scene, pseudo-labels are generated by following the same view rendering process as in the training phase and running them through the ensemble. The resulting 2D logits are back-projected to 3D and accumulated as votes. The final 3D mask is obtained by assigning the most voted class to each point. *Target Training Phase (red)*. Finally, a 3D model pretrained on the source dataset is fine-tuned on the pseudo-labels.

We propose a method that leverages aligned scenes to generate high quality pseudo-labels for the target domain, which are used to fine-tune a final 3D segmentation model pre-trained on the source domain. Our approach reaches state-of-the-art performance in UDA while introducing no computational overhead to the final 3D segmentation model. Our pseudo-label generation process belongs to the multi-view projection family of methods, where 3D scenes are analyzed via multiple 2D representations. We position virtual cameras around aligned Lidar scenes to generate rendered views (virtual camera images) from various

perspectives. While similar methods use real camera images for training and inference [8], we create large-scale synthetic 2D semantic segmentation datasets by rendering both the 3D scenes and their corresponding ground truth annotations. This eliminates the need for additional camera sensors and allows to freely choose the optimal parameters for selecting and rendering the views.

We demonstrate the effectiveness of our method for UDA in Real-to-Real tasks on the nuScenes (NS) [2] and SemanticKITTI (SK) [1] datasets (NS→SK and SK→NS), and in a Simulation-to-Real task on the SynLidar (SL) [29] dataset (SL→SK). We also demonstrate a potential application of our method to segment ‘rare classes’, where 3D annotations are not available for the desired target classes, but 2D annotations are available along with 3D annotations for other classes. Finally, we conduct a full ablation study to verify the importance of each component of our method. **Our main contributions are the following:**

- A method for Unsupervised Domain Adaptation in 3D semantic segmentation reaching state-of-the-art performance in  
nuScenes → SemanticKITTI and SemanticKITTI → nuScenes
- A novel multi-view projection framework for pseudo-label generation, with dataset generation capabilities
- A demonstration of an application of our method to segment ‘rare classes’ for which 3D annotations are not available

## 2 Related works

### 2.1 3D semantic segmentation

3D semantic segmentation is the task of assigning a semantic label to each point in a 3D point cloud. It is generally done either on Lidar point clouds [2,1], or RGB-D images [6]. Methods are usually divided in 3D-based and 2D-based. 3D models directly operate on the point cloud using 3D sparse convolutions [5], while 2D models re-use 2D image segmentation methods by projecting the point cloud to a 2D plane [14]. Importantly, LiDAR-based 3D semantic segmentation models are particularly sensitive to domain shift due to sensor-specific sampling and sparsity effects, often more so than 2D vision models [24,13].

2D approaches generally project the point cloud to a single 2D image with channels representing various features, e.g. height, intensity, density, etc. Various projection approaches exist, including Bird’s Eye View (BEV) [14] and Range View (RV) [28]. Multi-view projection methods try to leverage 2D models even further by repeatedly using the same model on multiple views of the 3D scene.

### 2.2 Multi-view projection for segmentation

The goal of multi-view projection methods is to extract as much knowledge from a 2D model as possible for 3D segmentation. This is done by inferring on multiple views of the 3D scene and then merging the resulting 2D segmentations. The problem then decomposes itself into two parts:

- P1. Which projections to use for the views and with which inference model?  
 P2. How to merge the 2D segmentation masks to get unique 3D labels?

Notice that the second problem is equivalent to the 2D-3D label propagation problem [27]. It is generally solved using either a voting scheme [12,17,3], where either the 2D masks or the probabilities/logits of the model are accumulated on points as votes, or with more complex methods such as Neural Networks [22,16,26].

Our proposed method uses a fast voting scheme on accumulated logits from a single 2D model.

In this paper, we focus on problem P1. Initially, [25] proposed multi-view projection for indoor RGB-D scenes, where the views are simply the RGB-D images themselves. For outdoor Lidar scenes, the same reasoning led [8] to use RGB camera images as views, with cameras calibrated to the Lidar [21]. However, this approach is limited as it requires using additional sensors, and the performance is tied to the quality of the sensor calibration. Mitigating this, [3] proposed to infer on rendered views of 3D scenes with an out-of-domain 2D model trained on camera images. This has the advantage of not requiring 3D labels or additional sensors, but comes with several limitations:

- The domain gap between camera images and views of Lidar point clouds is significant, which negatively impacts 2D model performance.
- The multi-view capability of the method is limited, as virtual camera placement must remain close to physically plausible viewpoints, e.g., those of real road users.
- Because aligning Lidar scans is essential for obtaining dense 3D scenes, the method is limited to static classes, as dynamic classes often appear with a so-called ‘*shadow effect*’ in the aligned scene, which is out of the camera images’ domain.

We propose to solve these three limitations by leveraging 3D annotations. This makes our method more dependent on 3D annotated data, but allows it to achieve significantly better performance and handle dynamic classes. Closest to our approach, [12] proposes to use 3D annotations to generate 2D synthetic datasets to train a 2D model for downstream multi-view projection for indoor RGB-D scenes. Our method distinguishes itself in its application to outdoor Lidar scenes, where much additional processing is required to obtain satisfying views, e.g. scan aligning, as well as in the choices for the feature rendering and view selection. We propose an ensembling mechanism for handling the modality choice. We also demonstrate the potential of such methods for pseudo-label generation for unsupervised domain adaptation.

### 2.3 Unsupervised Domain Adaptation

UDA aims to adapt a model trained on a labeled source domain  $(X_S, Y_S)$  to perform well on an unlabeled target domain  $X_T$ , where no ground-truth labels are available. Unlike supervised adaptation, only the source labels and unlabeled target samples  $X_{T\_train}$  can be exploited, while the evaluation is performed on a

disjoint set  $X_{T\_test}$ . This setting is particularly relevant for autonomous driving, where annotated data is costly to acquire, but raw scans from the deployment domain can be collected at scale.

We compare our approach to state-of-the-art UDA methods for 3D semantic segmentation, which mostly rely on self-training, temporal consistency, or compositional data augmentation. T-UDA [7] leverages temporal coherence by enforcing sequential point cloud consistency and cross-sensor geometric alignment within a mean-teacher framework. Lidar-UDA [24] simulates varying scan patterns via random beam dropping and improves pseudo-label reliability through cross-frame consistency and self-training. CoSMix [23] introduces compositional mixing across domains, generating hybrid point clouds to reduce the distribution gap between source and target. SALUDA [18] further improves self-training by enforcing domain-invariant geometric constraints on pseudo-labels. Finally, UniMix [30] extends mixing-based approaches with a unified framework that interpolates both features and labels across domains, enhancing robustness to domain shift.

Our method differs by relying entirely on a multi-view 2D projection pipeline to generate pseudo-labels for the target domain. These pseudo-labels are used to fine-tune a 3D segmentation model pretrained on the source domain. This approach reaches state-of-the-art performance in UDA.

### 3 Method

An overview of our method, which we call Seg3DbyPC2D, is shown in Fig. 1. To achieve UDA in 3D semantic segmentation, we simply pretrain a 3D model on the source dataset, then fine-tune it on the target dataset using pseudo-labels. Our main contribution is therefore our pseudo-label generation pipeline, which we describe in detail in this section.

In the following, we use the terms ‘*scene*’ to refer to a point cloud resulting from the accumulation of Lidar scans into a common frame, and ‘*view*’ to refer to a 2D image rendered from a 3D scene using a virtual camera.

#### 3.1 Pseudo-label Generation

Our method can be decomposed in the source training phase and the target inference phase. In both phases, we obtain 3D scenes and sample virtual camera poses to render views of the scenes. In the source training phase, we use these rendered views, along with rendered views of the 3D segmentation masks, to generate synthetic segmentation datasets (PC2D) that will be used to train an ensemble of 2D models. In the target inference phase, the views are used for inference with the previously trained ensemble of models, yielding pseudo-labels for the target domain. The choices of parameters for Virtual Camera Placement (VCP) and view rendering from Multiple Modalities (MMods) are crucial and are detailed in the following subsections. To obtain final pseudo-labels in the target domain, our multi-view projection approach is based on [3], which we improve with occlusion handling.

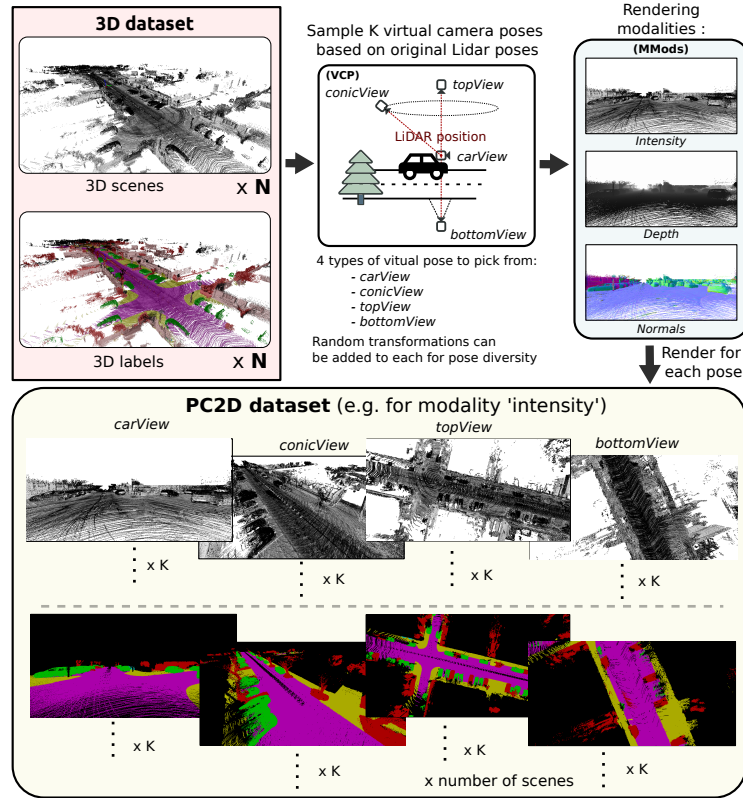


**Fig. 2. PointCloud2D (PC2D) dataset generation pipeline.** A 2D semantic segmentation dataset of rendered views of 3D point clouds is generated from a 3D semantic segmentation dataset. To obtain diverse images, virtual camera poses of 4 categories are sampled around the 3D scenes. The modality (colors) used for rendering can be chosen among sensor intensity, depth and projected normals. For each scene and each camera pose category, a large number of camera poses are sampled, and the corresponding 2D images and segmentation masks are rendered.

**Training with 3D annotations in 2D (PC2D)** A major contribution to our work compared to existing multi-view projection methods is the training of 2D models in *rendered view* domain. To that end, we generate large-scale synthetic datasets of 2D views of 3D scenes along with 2D segmentation masks, as shown in Fig. 2. We call these PC2D datasets.

Virtual camera poses are sampled arbitrarily around the 3D scene, which are then used to render 2D views. This way, we can generate an arbitrary number of (image, label) pairs, yielding large-scale datasets. Training on such datasets can be seen as a powerful data augmentation technique. The main limitation to this is that a limited number of annotated scenes will yield samples with less diversity as the total number of training samples increases.

The use of PC2D datasets allows to train the models in a *rendered view* source domain, very close to the target inference domain, yielding greater freedom over the view generation steps compared to existing methods. For example, generating bird’s eye view depth maps is possible, while views in [3], are limited to ‘road user viewpoint’ rendering of Lidar intensity. The two following subsections describe how we choose the virtual camera placement and the rendering modalities to obtain the best performance.

**Virtual Camera Placement** We propose to optimize the view generation by choosing relevant virtual camera poses.

After experimentation, we retain 4 types of camera poses based on the original Lidar sensor poses, which are already describing the trajectory of the ego vehicle along the scene. An illustration of the 4 types of camera pose is shown in Fig. 2, in the VCP module, and we describe them below:

- **carView**: The camera is placed at a road user’s perspective, i.e. at the approximate height of a car (random yaw can be applied).
- **conicView**: The camera is placed on the basis of a large imaginary cone pointing downwards, with the apex at the Lidar sensor position. The camera points to the apex of the cone. This corresponds to a ‘drone’ or ‘lamp post’ view of the scene, and is also the closest to the views that human annotators would typically use to annotate a scene.
- **topView**: The camera is placed directly above the Lidar position, looking downwards, with variable height and roll. This corresponds to the usual ‘bird’s eye view’ (BEV) of the scene.
- **bottomView**: The camera is placed under the scene, looking upwards. This is the opposite of a BEV. Rendering Lidar point clouds from below allows to clearly see the colors of the flat surfaces of the ground without occlusions from the objects above.

**Multi-Modalities** Similar to camera pose generation, PC2D datasets allow us to choose the visualization modality for the training and inference images, i.e. the rendered colors. While multi-view projections methods based on RGB cameras are limited to RGB colors, we can choose to render modalities such as Lidar intensity, depth maps, and normals. The final projection and voting step does not limit the number of votes, we therefore propose to train multiple models on multiple modalities, and use them together in an ensemble. We use the following modalities:

- **Intensities**: The Lidar sensor intensity, normalized by scan, following [3].
- **Depths**: The point cloud depth maps with respect to the camera pose.
- **Normals**: The components of the point cloud surface normals, computed using the normal estimation method in [9].

For each modality, we generate a PC2D dataset, and train a separate model. We then use ensembles of models to process each view of the scene at inference time.

**Projection and Fusion** To obtain final 3D segmentation masks from 2D models’ outputs, we use a similar projection step as in [3], where 2D logits are back-projected to 3D and accumulated as votes. We propose adding occlusion to the projection step (OCL). Naive back-projection from 2D to 3D suffers from points being included in the projection even if they are occluded by objects. We use depth maps generated from meshes, themselves generated using [9] for occlusion. Using meshes has the advantage of allowing less sparse depth maps which is more appropriate for dense point clouds. Finally, we set a margin parameter  $\delta = 0.5m$  to include points behind the depth map to account for the size of the occluding object. This final step yields the pseudo-labels for the target dataset.

## 4 Experiments

In this section we demonstrate the performance of our method for UDA on Lidar Semantic Segmentation tasks.

First, we show the performance of our method in both Real-to-Real and Simulation-to-Real settings. For both settings, we compare the results with the state-of-the-art methods in UDA. Then, we demonstrate how our method can be used to segment rare classes, for which 3D annotations are not available, by only using 2D annotations for those classes and 3D annotations for other classes. Finally, we conduct an ablation study to demonstrate the importance of each component of our method.

### 4.1 Datasets and Metrics

**Real-to-Real.** SemanticKITTI [1] (SK) and nuScenes [2] (NS) are two well-known large-scale datasets for AD, both providing and annotating Lidar 3D point clouds. The procedure generally adopted in the domain adaptation literature [10,11,7,24]

is to train on the official training splits for both datasets, e.g. 700 scenes for nuScenes and sequences 00 to 07, 09 and 10 for SemanticKITTI, and evaluate on the official validation splits, e.g. 150 scenes for nuScenes and sequences 08 for SemanticKITTI. We follow this procedure for comparing with the state of the art. Of the 700 nuScenes scenes, we use the 70 last scenes for validation. Similarly, we use sequence 10 of SemanticKITTI for validation. For the rare classes experiment 4.6 and the ablation study 4.5, we use a subset of the first 1800 scans from sequence 08 of the SK dataset for evaluation, to reduce the computational cost.

**Simulation-to-Real.** SynLidar [29] (SL) is a synthetic AD dataset captured with Unreal Engine 4. The sub-sampled version that is used in most of the literature [29,23,18,30] is composed of 13 sequences, containing 19,865 scans with annotations for 32 classes. No official validation split is provided, therefore we follow [10] and use sequences 05 and 10 for validation. We do not evaluate on SynLidar, as it is only used as a source dataset.

**Class mappings.** We evaluate two Real-to-Real settings, NS→SK and SK→NS, and one Sim-to-Real setting, SL→SK. To compare with the state-of-the-art, we follow [24,18] and use 10 classes common to NS and SK. For the SL→SK

scenario, we use the official SK19 class mapping as in [23,18]. To denote the different versions of the SemanticKITTI dataset, we use the following notations: SK<sub>10</sub>, SK<sub>19</sub>. The exact class mappings used can be found on github<sup>3</sup>.

**Metrics.** We measure the 3D semantic segmentation performance using the Intersection over Union (IoU) metric for all the experiments. We report both the per-class IoU and the mean IoU over all classes (mIoU). We compute all the metrics using code provided by [19], to ensure a fair comparison. For all UDA experiments, the evaluation is done with the 3D model after fine-tuning, to ensure similar conditions to the state-of-the-art methods, i.e. real-time inference on single scans. For the rare classes and ablation experiments, the evaluation is directly done on the pseudo-labels generated by the pipeline.

## 4.2 Implementation details

The most important hyper-parameters are presented in this section, but more details can be found on github<sup>3</sup>.

To begin with, we prepare the aligned scenes from SemanticKITTI and nuScenes. We use the already existing scenes from NS and accumulate scans 60 by 60 to create SK scenes. The intensities are normalized by scan, following [3].

NuScenes’ annotations are only available at 2Hz, while the scans are captured at 20Hz. To prepare for 2D segmentation label generation for PC2D datasets, we propagate the annotations to all points with a simple KNN method with  $K = 5$  to assign labels to each point in the dense scene.

The PC2D datasets are generated with 400,000 samples for each modality and source dataset. The views are uniformly sampled over the training scenes. For inference, we use 250 images per camera pose type, thus 1,000 images per scene, per modality. This amounts to 4,000 images total per scene. All views are rendered at 1024×512 resolution with a standard field of view. The inference time for each scene takes  $\sim 2$  minutes on a NVIDIA RTX 3070 GPU. This is however only done once for pseudo-label generation, and there is no overhead introduced to the final fine-tuned model in both memory and time.

For the back-projection step, we crop the projection outside a depth range of [1m, 30m], and when occlusion is used, we set the occlusion margin to  $\delta = 0.5m$  behind the depth encountered.

For the 2D segmentation models, we use the Mask2Former [4] model with Swin backbone [15], from the framework of [20]. We pretrain the model on the PC2D dataset for 70,000 iterations on 1024×512 resolution images with a batch size of 8. We use a fading learning rate of  $1e^{-4}$ .

For a fair comparison in UDA, we follow [7,24,18] and use as 3D model a MinkowskiNet 32 from [5] as the 3D segmentation model with the framework of [19]. We train it with the default settings from [19] for  $3 \times 12$  epochs on the source dataset, followed by 10,000 iterations with batch size 4 on the target pseudo-annotated dataset. The only augmentations used are basic random 3D flip, rotation, translation and scaling.

<sup>3</sup> <https://github.com/andrewcaunes/ia4markings>

NS→SK <sub>10</sub> (%IoU)	Car	Bicycle	Motorcycle	Truck	Other vehicle	Pedestrian	Driveable surf.	Sidewalk	Terrain	Vegetation	%mIoU
Source-only	74.1	0.0	10.2	1.1	1.0	4.4	63.4	31.8	36.0	25.6	24.8
T-UDA [7]	93.0	0.0	11.4	3.4	47.0	15.7	83.3	54.4	67.9	83.9	46.0
Lidar-UDA [24]	86.2	0.0	13.9	9.3	3.1	16.5	65.7	6.1	54.1	85.7	34.1
CoSMix [23]	77.1	10.4	20.0	15.2	6.6	51.0	52.1	31.8	34.5	84.8	38.3
SALUDA [18]	89.8	13.2	26.2	15.3	7.0	37.6	79.0	50.4	55.0	88.3	46.2
Ours	90.1	0.0	28.4	17.7	18.4	37.1	80.9	61.0	70.2	90.1	49.4

Table 1. UDA, NS→SK<sub>10</sub>. IoU per class and mIoU. Color: Best, Second.

SK <sub>10</sub> →NS (%IoU)	Car	Bicycle	Motorcycle	Truck	Other vehicle	Pedestrian	Driveable surf.	Sidewalk	Terrain	Vegetation	%mIoU
Source-only	1.8	0.0	0.0	0.0	0.0	0.5	6.7	0.1	0.1	0.3	0.9
T-UDA [7]	74.2	0.5	40.3	21.8	0.2	0.4	87.8	45.8	46.1	70.3	38.7
Lidar-UDA [24]	73.5	0.9	15.9	0.9	25.7	40.8	87.4	42.3	47.9	83.2	41.8
Ours	73.3	0.5	32.0	50.7	0.0	32.1	90.3	55.4	58.2	87.0	47.9

Table 2. UDA, SK<sub>10</sub>→NS. IoU per class and mIoU. Color: Best, Second.

### 4.3 Baselines

To demonstrate the capabilities of our method, we compare it to the state-of-the-art methods in UDA for 3D semantic segmentation. We use the results reported by the authors for each method, while ensuring a fair comparison by using the same dataset splits, class mappings, metrics and model architectures. For Real-to-Real, in the NS→SK<sub>10</sub> setting, we find the best performing methods to date are Lidar-UDA [24], T-UDA [7], CoSMix [23] and SALUDA [18]. In the SK<sub>10</sub>→NS setting, we compare with Lidar-UDA [24] and T-UDA [7], as CoSMix [23] and SALUDA [18] do not provide results for this setting. Note that T-UDA [7] also reports values for the *manmade* class, not reported by the other methods. We therefore do not include it and re-compute the mIoU accordingly. For Sim-to-Real, in the SL→SK<sub>19</sub> setting, we compare with SALUDA [18], CoSMix [23] and UniMix [30].

### 4.4 Unsupervised Domain Adaptation Results

**Real-to-Real setting** Results for the NS→SK<sub>10</sub> setting can be found in Table 1. This UDA setting is particularly challenging as the source (NS) uses a 32-beam

SL→SK <sub>19</sub> (% IoU)	Car	Bicycle	Motorcycle	Truck	Other vehicle	Pedestrian	Bicyclist	Motorcyclist	Road	Parking	Sidewalk	Other ground	Building	Fence	Vegetation	Trunk	Terrain	Pole	Traffic sign	% mIoU
Source-only	50.8	7.6	11.8	1.4	3.2	15.8	34.8	3.9	30.0	4.5	34.5	0	27.0	15.8	62.9	24.4	43.0	18.9	6.4	20.9
CoSMix [23]	75.1	6.8	29.4	27.1	11.1	22.1	25.0	24.7	79.3	14.9	46.7	0.1	53.4	13	67.7	31.4	32.1	37.9	13.4	32.2
SALUDA [18]	67.0	7.7	14.4	1.3	5.2	24.1	52.6	2.7	52.5	10.5	44.1	0.4	51.8	13.6	69.7	40.5	56.5	45.0	14.3	30.2
Unimix [30]	80.3	6.1	32.5	29.2	10.6	23.7	30	24.5	62.2	15.9	46.5	0.1	60.9	15.8	70.7	34.9	41.2	38.6	17.1	33.7
Ours	83.5	0.9	6	10.4	3.0	19.8	13.5	0.2	80.2	0.0	51.6	0	78.8	16.7	51.9	32.0	36.8	40.6	10.1	28.2

Table 3. UDA, SL→SK<sub>19</sub>. IoU per class and mIoU. Color: Best, Second.

Lidar, less dense than the 64-beam Lidar used in the target (SK). Seg3DbyPC2D is able to outperform the state-of-the-art by +3.2 mIoU points. Interestingly, our method reaches state-of-the-art performance even for dynamic classes such as *car*, *motorcycle* and *truck*. This demonstrates that the model learns to match ‘*shadow effect*’-like features with the corresponding classes.

Results for the SK<sub>10</sub>→NS setting can be found in Table 2. In this setting, Seg3DbyPC2D is even more dominant, with a +6.1 mIoU advantage over state-of-the-art. The method results in particularly strong performance on static classes such as *driveable surface*, *sidewalk*, *terrain* and *vegetation*, which can be explained by the higher difficulty to segment dynamic classes displaying some ‘*shadow effect*’. For both tasks, we notice relatively lower performance on small classes, such as *bicycle* and *pedestrian*, which might be due to the projection errors caused by poor sensor calibration being more important for small objects.

**Simulation-to-Real setting** Table 3 reports the results for the SL→SK<sub>19</sub> setting. Overall, our method achieves lower mIoU compared to prior works such as CoSMix [23], SALUDA [18], and UniMix [30]. However, it consistently performs strongly on several static classes, notably, *road* (80.2), *sidewalk* (51.6), and *building* (78.8), and some dynamic classes such as *car* (83.5), where it reaches state-of-the-art performance. This suggests that the projection-based pseudo-labeling is particularly effective on large, well-structured classes but less robust on fine-grained or rare classes such as *bicycle*, *motorcycle*, and *motorcyclist*. While the global mIoU is lower (28.2), the results highlight that our approach can still surpass prior methods on key static categories, underlining its strength for Sim-to-Real in some applications such as road infrastructure analysis.

#### 4.5 Ablation Study

We conduct a complete ablation study to verify the importance of each component of our method. Results can be seen in Table 4. The first stage (a) corresponds to the base multi-view projection method that we followed from [3]. We add the PC2D dataset training in stage (b), the occlusion handling in stage (c), the Virtual Camera Placement in stage (d), and the full Seg3DbyPC2D with the

Multi-Modalities module is evaluated in stage (e). We evaluate the models in both  $SK_{10} \rightarrow SK_{10}$  (in-domain) and  $NS \rightarrow SK_{10}$  (UDA).

	PC2D	OCL	VCP	MMods	$SK_{10}$	$\nearrow_{mIoU}$	NS	$\nearrow_{mIoU}$
(a)					15	-	15	-
(b)	✓				31.1	+16.1	28.9	+13.9
(c)	✓	✓			42.0	+10.9	34.4	+5.5
(d)	✓	✓	✓		43.7	+1.7	34.3	-0.1
(e)	✓	✓	✓	✓	49.3	+5.6	40.9	+6.6

**Table 4. Ablation study.** (f) is full Seg3DbyPC2D . (a) is [3]. Models are all evaluated on  $SK_{10}$ . Datasets indicated for the results columns are the training datasets. Results are in % mIoU.

We see that the addition of the PC2D dataset leads to the most significant improvement, followed by the occlusion handling and the multi-modalities module. Interestingly, the addition of the VCP module leads to an improvement only for the  $SK_{10} \rightarrow SK_{10}$  setting, and not for UDA. This might be because using more diverse camera poses increases the risk of encountering a large domain shift within one camera pose type, e.g. the difference in Lidar point density might yield a larger difference in BEV type views than in *road user* type views, since the difference in point density becomes significant when seen from afar.

Overall, all components proposed in our method seems valuable for either supervised or UDA applications.

#### 4.6 Application to rare classes

A common real world scenario in 3D semantic segmentation is to have access to 3D annotations for some classes in a source domain, but not the desired target classes. However, 2D annotations are more generally available as they are less costly. For such a situation when 2D annotations of the target classes are available, [3] proposes a multi-view projection method with 2D models trained on real camera images, which then perform out-of-domain inference on virtual rendered views. We show that our method can help to significantly improve the performance of this approach by using the 3D annotations and our PC2D dataset generation pipeline to pretrain the 2D model in rendered view domain. The model is then fine-tuned on real camera images with annotations for the target classes. The pretraining on 3D annotations allows to significantly bridge the domain gap that exists at inference time by first exposing the model to rendered images.

**Experimental setup** For this experiment, 3 datasets are used:

- A *pretraining* 3D source dataset, with 3D annotations for any classes (but not the target classes). We use nuScenes (NS) [2].

Method	traffic sign	$\nearrow_{mIoU}$
Baseline [3]	11.9	
Seg3DbyPC2D (ours)	<b>18.3</b>	<b>+6.4 (+53%)</b>

**Table 5. Application to rare classes.** IoU on SemanticKITTI for the ‘traffic sign’ class.

- A *rare classes* 2D dataset, with 2D annotations for the desired target classes. We use Mapillary Vistas (MV) [21], using only the *traffic sign* class as the target class.
- A *target* 3D dataset. We use SemanticKITTI (SK) [1], as it conveniently provides 3D annotations for our target class, *traffic sign*, which will allow to perform a quantitative evaluation.

We compare our Seg3DbyPC2D with the baseline from [3], both trained on the *rare classes* dataset. Differently from [3] and from our base method in Sec. 3, we use the RGB colorized point clouds using camera images for SK and NS as the rendered views’ modality instead of Lidar intensities or other modalities. This reduces the domain gap with the real camera images of the *rare classes* dataset, but requires that camera data be available for the *pretraining* dataset. We use Mask2Former models for both methods with the same parameters as 4.2. For Seg3DbyPC2D, we pretrain the 2D model on a PC2D dataset, generated from the *pretraining* dataset, as in 4.2, and then fine-tune the model on the *rare classes* dataset for 10,000 iterations, while freezing the first block of the Swin backbone.

**Results** Table 5 reports the results as computed on SK for the *traffic sign* class. We see a significant improvement over the base method, with a +6.4 mIoU improvement, corresponding to relative increase of +53%. This shows that our method can be used to segment rare classes for which 3D annotations are not available, when some 2D annotations are available.

## 5 Conclusion

We have presented a new UDA method based on a novel multi-view projection framework for 3D semantic segmentation. After generating large-scale synthetic 2D datasets (PC2D) from aligned Lidar scenes in the source domain to train an ensemble of 2D segmentation models, our method leverages occlusion-aware back-projection and voting to produce high-quality 3D pseudo-labels for the target domain.

Extensive experiments demonstrate that our approach achieves state-of-the-art performance in Real-to-Real UDA and useful performance for large classes in Sim-to-Real UDA. We also demonstrated a potential application of our method to segment rare classes with no 3D annotations but 2D annotations available.

While our approach thoroughly explored problem 1) mentioned in Section 2.2 of what views to use for inference, and which models to infer with, future research could be led to explore problem 2) of how to optimally use the numerous outputs from the ensemble of models on all views to assign final 3D labels. In particular, our logits accumulation and voting scheme does not use important information such as spatial proximity of the points or class size statistics. Information like this could be used to train a model to output the final 3D segmentation mask with more insight than a simple voting scheme.

We hope that our work will inspire further research into this direction.

## References

1. Behley, J., Garbade, M., Milioto, A., Quenzel, J., Behnke, S., Stachniss, C., Gall, J.: SemanticKITTI: A Dataset for Semantic Scene Understanding of LiDAR Sequences (Aug 2019). <https://doi.org/10.48550/arXiv.1904.01416>, arXiv:1904.01416 [cs]
2. Caesar, H., Bankiti, V., Lang, A.H., Vora, S., Liong, V.E., Xu, Q., Krishnan, A., Pan, Y., Baldan, G., Beijbom, O.: nuScenes: A multimodal dataset for autonomous driving (May 2020). <https://doi.org/10.48550/arXiv.1903.11027>, arXiv:1903.11027 [cs, stat]
3. Caunes, A., Chateau, T., Frémont, V.: 3D Can Be Explored In 2D : Pseudo-Label Generation for LiDAR Point Clouds Using Sensor-Intensity-Based 2D Semantic Segmentation. In: 2024 IEEE Intelligent Vehicles Symposium (IV). pp. 2192–2197 (Jun 2024). <https://doi.org/10.1109/IV55156.2024.10588443>, iSSN: 2642-7214
4. Cheng, B., Misra, I., Schwing, A.G., Kirillov, A., Girdhar, R.: Masked-attention Mask Transformer for Universal Image Segmentation (Jun 2022). <https://doi.org/10.48550/arXiv.2112.01527>, arXiv:2112.01527 [cs]
5. Choy, C., Gwak, J., Savarese, S.: 4D Spatio-Temporal ConvNets: Minkowski Convolutional Neural Networks (Jun 2019), arXiv:1904.08755 [cs] version: 4
6. Dai, A., Chang, A.X., Savva, M., Halber, M., Funkhouser, T., Nießner, M.: ScanNet: Richly-annotated 3D Reconstructions of Indoor Scenes (Apr 2017). <https://doi.org/10.48550/arXiv.1702.04405>, arXiv:1702.04405
7. Gebrehiwot, A.H., Hurych, D., Zimmermann, K., Pérez, P., Svoboda, T.: T-UDA: Temporal Unsupervised Domain Adaptation in Sequential Point Clouds. In: 2023 IEEE/RSJ International Conference on Intelligent Robots and Systems (IROS). pp. 7643–7650 (Oct 2023). <https://doi.org/10.1109/IROS55552.2023.10341446>, iSSN: 2153-0866
8. Genova, K., Yin, X., Kundu, A., Pantofaru, C., Cole, F., Sud, A., Brewington, B., Shucker, B., Funkhouser, T.: Learning 3D Semantic Segmentation with only 2D Image Supervision (Oct 2021). <https://doi.org/10.48550/arXiv.2110.11325>, arXiv:2110.11325 [cs]
9. Huang, J., Gojcic, Z., Atzmon, M., Litany, O., Fidler, S., Williams, F.: Neural Kernel Surface Reconstruction (Jun 2023), arXiv:2305.19590 [cs]
10. Kim, H., Kang, Y., Oh, C., Yoon, K.J.: Single Domain Generalization for LiDAR Semantic Segmentation. In: 2023 IEEE/CVF Conference on Computer Vision and Pattern Recognition (CVPR). pp. 17587–17598. IEEE, Vancouver, BC, Canada (Jun 2023). <https://doi.org/10.1109/CVPR52729.2023.01687>
11. Kim, J., Woo, J., Kim, J., Im, S.: Rethinking LiDAR Domain Generalization: Single Source as Multiple Density Domains (Jul 2024). <https://doi.org/10.48550/arXiv.2312.12098>, arXiv:2312.12098 [cs]

12. Kundu, A., Yin, X., Fathi, A., Ross, D., Brewington, B., Funkhouser, T., Pantofaru, C.: Virtual Multi-view Fusion for 3D Semantic Segmentation. vol. 12369, pp. 518–535. Springer International Publishing, Cham (2020). [https://doi.org/10.1007/978-3-030-58586-0\\_31](https://doi.org/10.1007/978-3-030-58586-0_31), book Title: Computer Vision – ECCV 2020 Series Title: Lecture Notes in Computer Science
13. Lambert, J., Liu, Z., Sener, O., Hays, J., Koltun, V.: MSeg: A Composite Dataset for Multi-Domain Semantic Segmentation
14. Lang, A.H., Vora, S., Caesar, H., Zhou, L., Yang, J., Beijbom, O.: PointPillars: Fast Encoders for Object Detection from Point Clouds (Dec 2018)
15. Liu, Z., Lin, Y., Cao, Y., Hu, H., Wei, Y., Zhang, Z., Lin, S., Guo, B.: Swin Transformer: Hierarchical Vision Transformer using Shifted Windows (Aug 2021). <https://doi.org/10.48550/arXiv.2103.14030>, arXiv:2103.14030 [cs]
16. Ma, L., Stückler, J., Kerl, C., Cremers, D.: Multi-View Deep Learning for Consistent Semantic Mapping with RGB-D Cameras (Dec 2017). <https://doi.org/10.48550/arXiv.1703.08866>, arXiv:1703.08866 [cs]
17. McCormac, J., Handa, A., Davison, A., Leutenegger, S.: SemanticFusion: Dense 3D Semantic Mapping with Convolutional Neural Networks (Sep 2016). <https://doi.org/10.48550/arXiv.1609.05130>, arXiv:1609.05130 [cs]
18. Michele, B., Boulch, A., Puy, G., Vu, T.H., Marlet, R., Courty, N.: SALUDA: Surface-based Automotive Lidar Unsupervised Domain Adaptation (Nov 2023), arXiv:2304.03251 [cs]
19. MMDetection3D Contributors: OpenMMLab’s Next-generation Platform for General 3D Object Detection (Jul 2020), original-date: 2020-07-08T03:39:45Z
20. MMSegmentation Contributors: OpenMMLab Semantic Segmentation Toolbox and Benchmark (Jul 2020), original-date: 2020-06-14T04:32:33Z
21. Neuhold, G., Ollmann, T., Bulo, S.R., Kotschieder, P.: The Mapillary Vistas Dataset for Semantic Understanding of Street Scenes. In: 2017 IEEE International Conference on Computer Vision (ICCV). pp. 5000–5009. IEEE, Venice (Oct 2017). <https://doi.org/10.1109/ICCV.2017.534>
22. Robert, D., Vallet, B., Landrieu, L.: Learning Multi-View Aggregation In the Wild for Large-Scale 3D Semantic Segmentation (Jul 2022). <https://doi.org/10.48550/arXiv.2204.07548>, arXiv:2204.07548 [cs]
23. Saltori, C., Galasso, F., Fiameni, G., Sebe, N., Poiesi, F., Ricci, E.: Compositional Semantic Mix for Domain Adaptation in Point Cloud Segmentation. *IEEE Transactions on Pattern Analysis and Machine Intelligence* **45**(12), 14234–14247 (Dec 2023). <https://doi.org/10.1109/TPAMI.2023.3310261>
24. Shaban, A., Lee, J., Jung, S., Meng, X., Boots, B.: LiDAR-UDA: Self-ensembling Through Time for Unsupervised LiDAR Domain Adaptation. In: 2023 IEEE/CVF International Conference on Computer Vision (ICCV). pp. 19727–19737 (Oct 2023). <https://doi.org/10.1109/ICCV51070.2023.01812>, iSSN: 2380-7504
25. Su, H., Maji, S., Kalogerakis, E., Learned-Miller, E.: Multi-view Convolutional Neural Networks for 3D Shape Recognition (Sep 2015). <https://doi.org/10.48550/arXiv.1505.00880>, arXiv:1505.00880 [cs]
26. Wang, B., Chao, W.L., Wang, Y., Hariharan, B., Weinberger, K., Campbell, M.: LDLS: 3-D Object Segmentation Through Label Diffusion From 2-D Images (Oct 2019)
27. Wang, Y., Ji, R., Chang, S.F.: Label Propagation from ImageNet to 3D Point Clouds
28. Wu, B., Zhou, X., Zhao, S., Yue, X., Keutzer, K.: SqueezeSegV2: Improved Model Structure and Unsupervised Domain Adaptation for Road-Object Segmentation

- from a LiDAR Point Cloud. In: 2019 International Conference on Robotics and Automation (ICRA). pp. 4376–4382 (May 2019). <https://doi.org/10.1109/ICRA.2019.8793495>, ISSN: 2577-087X
29. Xiao, A., Huang, J., Guan, D., Zhan, F., Lu, S.: Transfer Learning from Synthetic to Real LiDAR Point Cloud for Semantic Segmentation (Dec 2021). <https://doi.org/10.48550/arXiv.2107.05399>, arXiv:2107.05399 [cs]
  30. Zhao, H., Zhang, J., Chen, Z., Zhao, S., Tao, D.: UniMix: Towards Domain Adaptive and Generalizable LiDAR Semantic Segmentation in Adverse Weather (Apr 2024). <https://doi.org/10.48550/arXiv.2404.05145>, arXiv:2404.05145 [cs]